ANNALS OF GEOPHYSICS, 68, 5, DM557, 2025; doi:10.4401/ag-9327
OPEN ACCESS

Northern Promontory of AdriaArray: Network Design and Realization

Luděk Vecsey[*,1], Piotr Środa[2], Jaroslava Plomerová[1], Götz Bokelmann[3], Monika Bociarska[2], Kristian Csicsay[4], Wojciech Czuba[2], Lucia Fojtíková[4,5], Petr Jedlička[1], Hana Kampfová Exnerová[1], Petr Kolínský[1], Josef Kotek[1], Szymon Malinowski[6], Maciej Mendecki[7], Julia Rewers[2], Daniel Schützenhofer[3]

(1) Institute of Geophysics of the Czech Academy of Sciences, Prague, Czech Republic
(2) Institute of Geophysics, Polish Academy of Sciences, Warsaw, Poland
(3) Department of Meteorology and Geophysics, University of Vienna, Austria
(4) Earth Science Institute of the Slovak Academy of Sciences, Bratislava, Slovakia
(5) Institute of Rock Structure and Mechanics of the Czech Academy of Sciences, Prague, Czech Republic
(6) Institute of Geophysics, Faculty of Physics, University of Warsaw, Poland
(7) Institute of Earth Sciences, Faculty of Natural Sciences, University of Silesia in Katowice, Poland

Article history: received March 5, 2025; accepted October 30, 2025

Abstract

The northern extension of the AdriaArray, a dense network of broadband seismic stations, covers the southeastern part of the Bohemian Massif, the Eastern Alps, the Western Carpathians, and the northernmost part of the Pannonian Basin. Considering also the previous passive experiments carried out since 2015, the existing 32 broadband permanent stations have been complemented by 89 temporary stations deployed in the collaborative effort of institutions from the Czech Republic, Poland, Austria, and Slovakia. We document the seismic station configuration, instrumental equipment, data transmission, preprocessing, and availability, as well as the general organization of the network. Since spring 2022, when the AdriaArray network started its operation, to January 2025, approximately 2.8 TB of data recorded by the temporary stations has been transmitted to the European Integrated Data Archive (EIDA), with an average completeness of 80% and real-time operation for 91% of the stations. The network records valuable data for a wide range of Earth science studies, including earthquake location, seismic hazard assessment, and high-resolution images of the crust and upper mantle structure. As examples of data utilization, we show Moho depth variations from the Bohemian Massif to the West Carpathians and the northernmost part of the Pannonian Basin, as well as prevailing NW-SE polarization azimuths of the fast shear waves from the splitting evaluations at stations in the broader surroundings of the Carpathians.

Keywords: AdriaArray; Temporary seismic network; MOBNET pool; Central Europe; Seismic noise level

1. Introduction

The seismic stations described in this paper represent the northern extension of the large-scale, multinational AdriaArray (AdA) network, which covers southeastern Europe (Kolínský et al., 2025a). The AdriaArray project is designed to study the complex tectonics and dynamics of the Adriatic microplate and its relatively large surroundings including the deformed parts of Adria and Eurasia bordered by undeformed Eurasia and Africa (Faccenna et al., 2014). The Adria is an elongated disappearing plate surrounded by lithospheric slabs and subduction zones (e.g., Schmid et al., 2020; van Hinsbergen et al., 2020; Kissling, 2024). Important structural targets are the 3D geometries of the slabs and their mechanical connection with the plates. The attachment of a slab to the sub-horizontal lithosphere, slab tears, and slab break-off are among the primary discussion topics of orogen evolution in the convergence belt around Adria (Handy et al., 2019; Kästle et al., 2020). The AdA project deals with interactions of the Adria with adjacent plates and concentrates on processes governing plate deformation, driving forces and implications for seismicity, volcanism, and geohazard in southeastern Europe. For a detailed description of the scopes and objectives of the AdA project, we refer to Kolínský et al. (2025a).

Our target region extends from the southeastern part of the Bohemian Massif and the Eastern Alps in the west, through the Vienna Basin to the Western Carpathian mountain ranges and the northernmost part of the Pannonian Basin in the east. This sector has been monitored by the previous AlpArray Seismic Network (2016-2019), the PACASE network (2019-2022), and the subsequent AdriaArray network discussed in this paper (Fig. 1). The region is geologically diverse, featuring a mix of Variscan units and young Alpine orogenic structures and basins. The Eastern Alps, the easternmost segment of the Alpine chain, underwent significant post-orogenic tectonic reorganization during the Neogene (Handy et al., 2015). The arcuate geometry is characteristic of the Carpathians

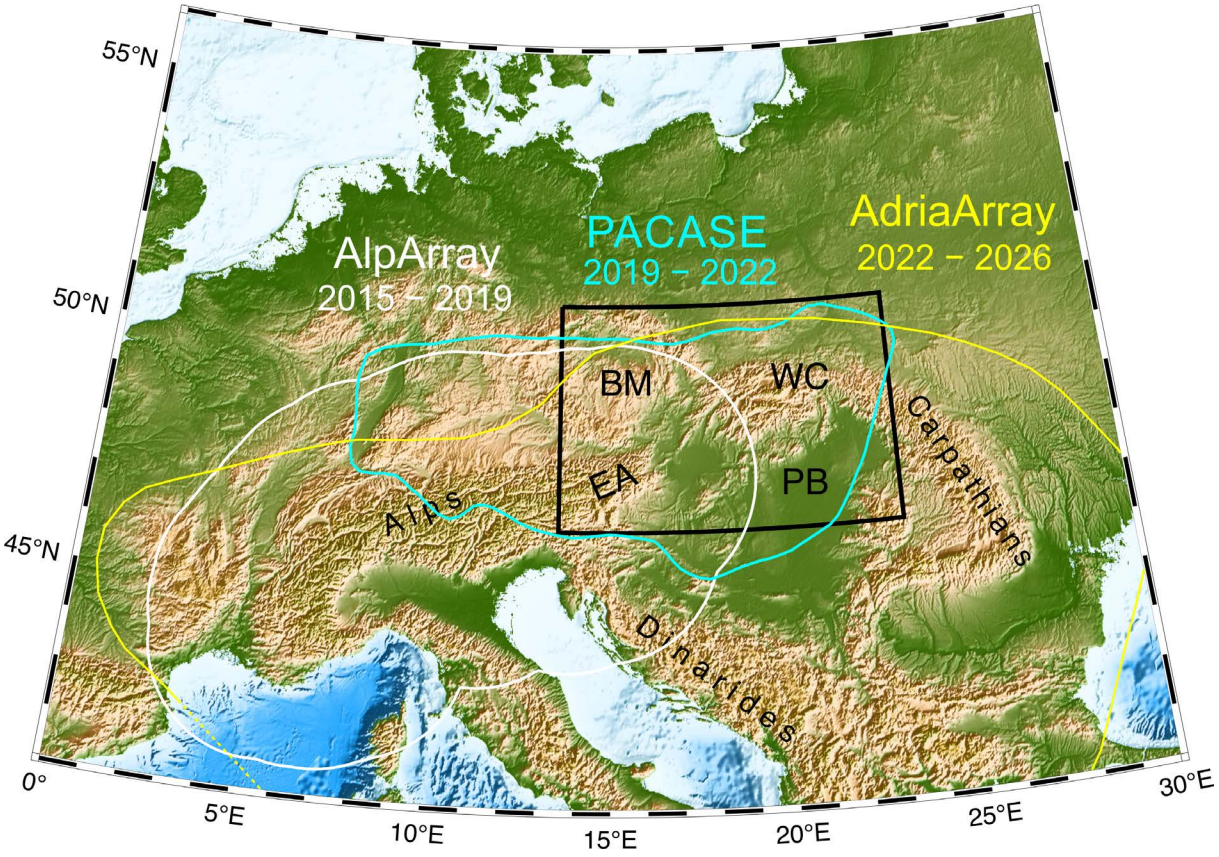

Figure 1. Topography of Europe (Tozer et al., 2019) with a black frame marking the northern promontory of the AdriaArray network covering the southeastern part of the Bohemian Massif (BM), Eastern Alps (EA), Western Carpathians (WC), Vienna, and the northernmost part of the Pannonian Basins (PB). Areas of the previous AlpArray Seismic Network (2016-2019) and PACASE network (2019-2022), and the current AdriaArray network (2022-2026) are contoured in white, cyan, and yellow, respectively.

surrounding most of the Pannonian Basin. The Western Carpathians were shaped by both compressional forces and subsequent extensional reactivation, as evidenced by their structural evolution and metamorphic patterns. They display a more complex nappe structure compared to the Alps, with ongoing research focusing on the role of micro-continental blocks and the evolution of the Carpathian orocline (Hók et al., 2014; Golonka et al., 2019). The Bohemian Massif, situated north of the Eastern Alps, represents the largest Variscan massif in Central Europe. The region's proximity to the Alpine and Carpathian orogens creates a unique setting for studying lithospheric interactions, including deformation at lithospheric margins and intraplate seismicity (Hetényi et al., 2018b). Altogether, these geological features make the Eastern Alps, Western Carpathians, Pannonian Basin, and the eastern rim of the Bohemian Massif an ideal setting for studying plate collision, subduction processes, and lithosphere deformation and dynamics. The evolution of the region, shaped by interactions between basins, orogens, and microplates, provides a compelling natural laboratory for addressing geodynamic questions (e.g., Schmid et al., 2020; Kissling, 2024; Kolínský et al., 2025a).

This region holds significant value for studies of the Earth's crust, lithosphere, and upper mantle structure by advanced seismological methods. These include primarily body and surface wave tomography, ambient noise imaging, and seismicity analysis, complemented by joint inversions integrating seismological and potential field data, and many others. Research goals also encompass monitoring seismic activity and interpreting it within the framework of seismotectonics and geodynamics.

Seismic hazard in the Western Carpathians and Pannonian Basin is relatively low in comparison with the hazard in the Southern Carpathians (Vrancea region). The peak ground acceleration (PGA) does not exceed 0.1 g according to the ESHM20 model (Danciu et al., 2021) for the broader W. Carpathian region (Fig. 2). However, there are some seismic events in the Eastern Alps, Little Carpathians, or in eastern Slovakia, with magnitudes Mw 5

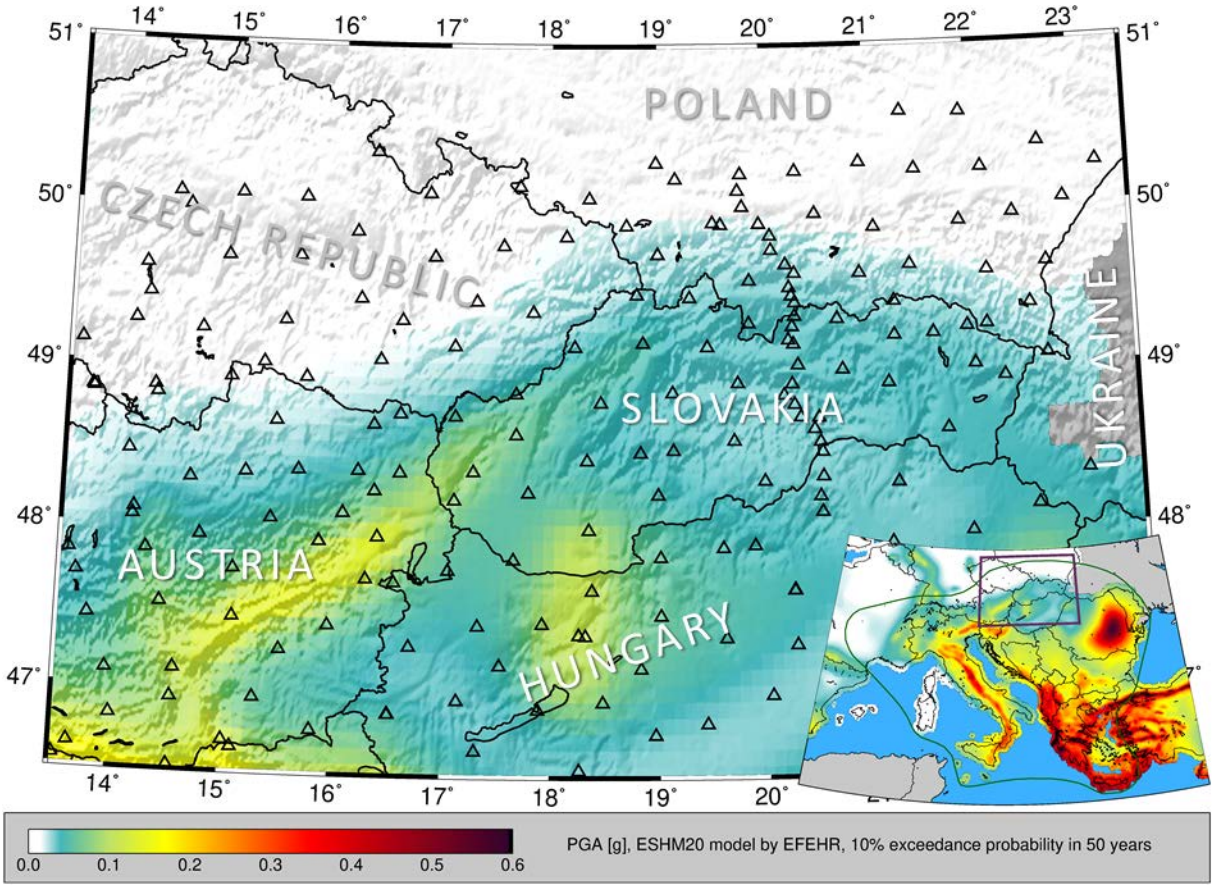

Figure 2. Seismic hazard displayed as peak ground acceleration (PGA) in [g] for a 10% exceedance probability in 50 years, based on the 2020 European Seismic Hazard Model (ESHM20) by European Facilities for Earthquake Hazard and Risk (EFEHR) (Danciu et al., 2021). Black triangles mark all seismic stations contributing to the AdriaArray network. A small inset map shows the seismic hazard across the entire AdriaArray region.

(Cipciar et al., 2025). Though the seismicity is weak, understanding the seismic regime of the region remains essential for hazard assessments and regional planning of constructions, especially for power plants and other large industrial constructions.

This paper provides a comprehensive overview of the deployment and operation of temporary seismic stations in the northern part of the AdriaArray network during the period May 2022-January 2025 (Fig. 3). We describe in detail the design, technical specifications and geographical locations of the stations, and acknowledge the collaborative contributions of six institutions deploying and operating the stations: Institute of Geophysics of the Czech Academy of Sciences (IG CAS), Institute of Geophysics of the Polish Academy of Sciences (IG PAS), University of Warsaw, University of Silesia in Katowice (Poland), University of Vienna (IMGW), Austria and Earth Science Institute of the Slovak Academy of Sciences (ESI SAS).

2. Network layout and instrument equipment

The AdriaArray network (Fig. 3, inset) covers the Adriatic region and adjacent areas in southeastern Europe by densely distributed broadband seismic stations. The installation of temporary stations, in combination with existing permanent networks, aims at recording a sufficient number of seismic waveforms for imaging crustal and mantle structures, monitoring seismicity, and addressing regional geodynamic questions.

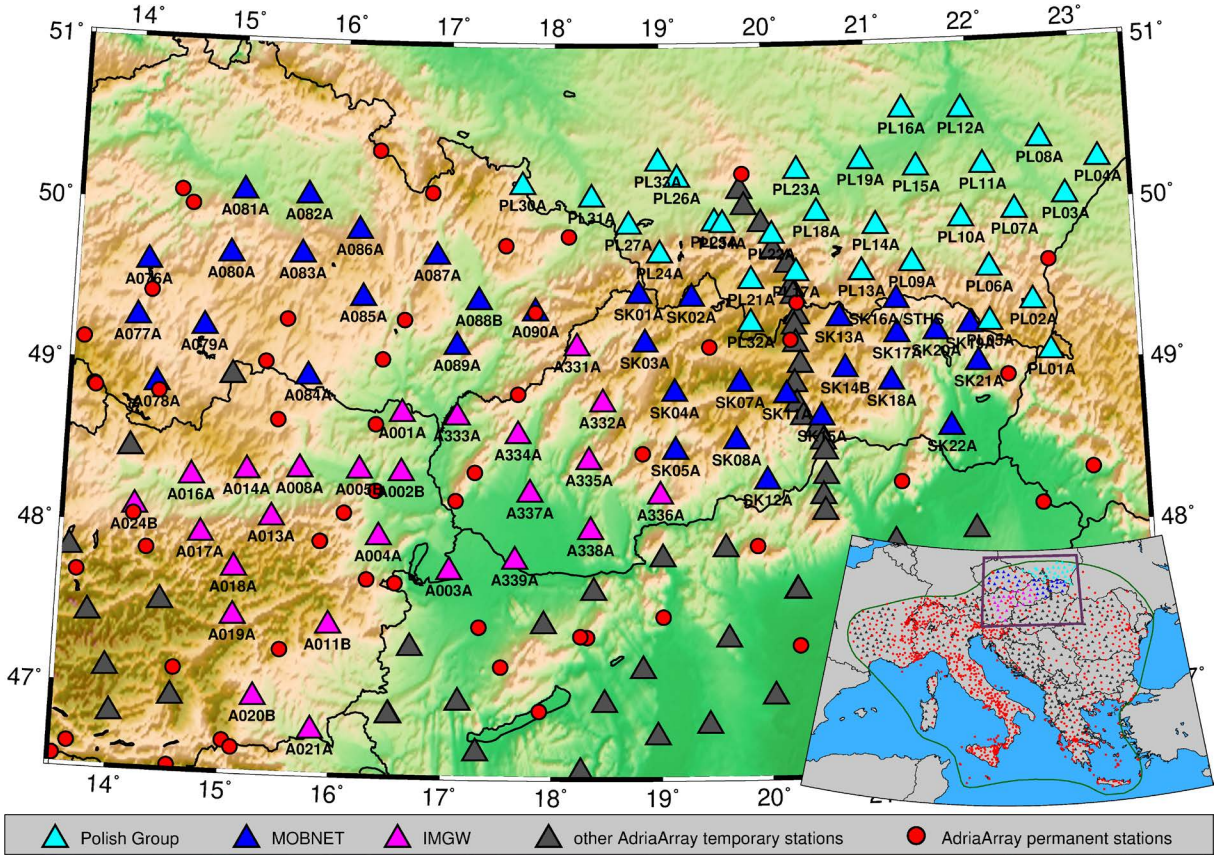

Figure 3. Distribution of seismic stations in the northern part of the AdriaArray network. The colored triangles mark the temporary stations of the Polish institutions (cyan), stations from the Czech MOBNET pool (blue), and stations from the University of Vienna (IMGW), Austria (magenta). Black triangles and red circles mark temporary seismic stations of other institutions contributing to the AdriaArray network and permanent stations in the region, respectively. The north-south transect, spanning from Poland through Slovakia to Hungary, is operated by the Carpathian Project Group and was designed to provide structural details across the key tectonic structures of the region (Soni et al., 2025). The ETOPO Global Relief Model data are provided by the NOAA Physical Sciences Laboratory (Amante and Eakins, 2009).

The northern part of AdA is located in four central European countries – the south-eastern part of the Czech Republic, Slovakia, southern Poland, and northeastern Austria (Fig. 3), and benefits significantly from previous passive experiments, particularly the AlpArray (Hetényi et al., 2018a) and PACASE (Schlömer et al., 2024). The temporary stations operating currently in the northern AdA region have been involved in the previous experiments mentioned above. Therefore, the inter-station distance follows that of the AlpArray and PACASE experiments, with a median value of 31 km. For a detailed description of the continuity between the previous projects and the AdriaArray initiative, see Kolínský et al. (2025a).

Before the realization of the experiments, only 32 permanent stations with network codes CZ (Institute of Geophysics of the Czech Academy of Sciences (CAS) et al., 1973), SK (ESI SAS; former GPI SAS (Geophysical Institute of the Slovak Academy of Sciences), 2004), PL (Institute of Geophysics, Polish Academy of Sciences, 1990), and OE (ZAMG – Zentralanstalt für Meteorologie und Geodynamik, 1987) operated in the region. The deployment of 89 temporary stations has significantly increased the density of seismic broadband receivers in the northern AdriaArray region. The temporary stations, provided by various institutions, consist of different types of broadband seismometers and dataloggers, but all sensors guarantee corner periods within the range of 30 seconds to 120 seconds (see Fig. 4).

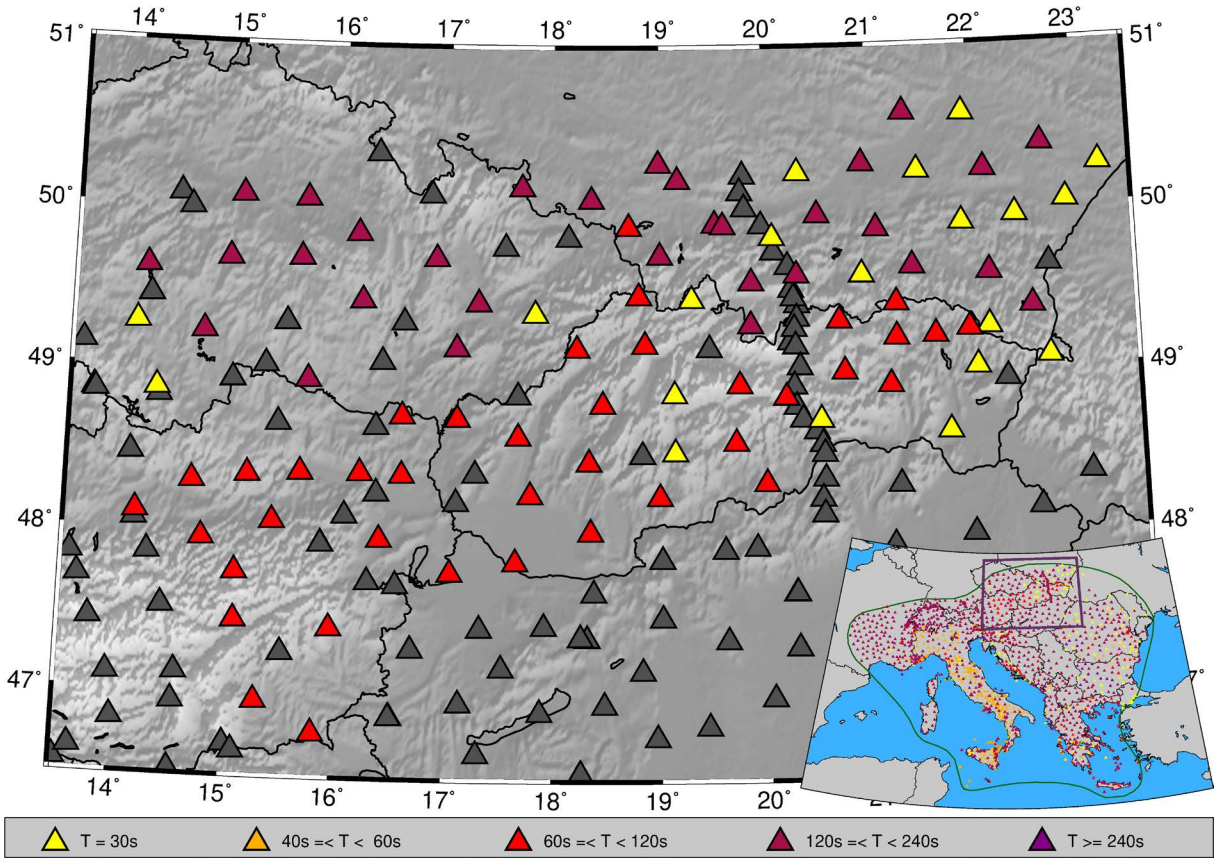

Figure 4. Temporary seismic stations in the northern part of the AdriaArray color-coded according to the sensor corner periods.

2.1 Temporary stations of the MOBNET pool deployed in Czechia and Slovakia

The Institute of Geophysics of the Czech Academy of Sciences contributes to the AdriaArray project with 52 broadband seismic stations from its MOBNET pool (Plomerová, 2025). Eight of these stations are deployed in Romania (Borleanu et al., 2025) and ten stations in Bulgaria (Kampfová Exnerová et al., 2025). In this work, we describe the deployment and operation of 34 stations in the Czech Republic and Slovakia (Fig. 3). Temporary stations installed in the Czech Republic, formerly within the framework of the AlpArray project (Hetényi et al., 2018a; Vecsey et al., 2017), became a part of one of its complementary projects, PACASE (2019-2022). During this period,

the stations retain their original AlpArray network code Z3 (AlpArray Seismic Network, 2015). In 2022, 15 of these stations, with names ranging from A076 to A090, were incorporated into the AdriaArray under the network code Z6 (Schlömer et al., 2022). Station A078A was later dismounted and its function was taken over by the nearby permanent station CKRC, and station A090A was transformed into permanent station MAUC, both in the Czech Regional Seismic Network (CRSN, network code CZ; see Table S1 in the Supplement).

Similarly, two network codes were used sequentially for the MOBNET stations operating in central and eastern Slovakia. These stations were installed in 2019 for the PACASE experiment with network code ZJ (Hetényi et al., 2019; Schlömer et al., 2024). In May 2022, when they became part of the AdriaArray, the code changed to Z6, and the PACASE station SK06A was replaced by the upgraded permanent broadband station LANS of the National Network of Seismic Stations (NNSS, network code SK).

The site selection for the temporary stations followed several criteria. Besides the homogeneous distribution of stations with the defined inter-station distance, we sought low-noise environments suitable for broadband observations. This was particularly challenging in densely populated and industrial regions. Preferred sites provided both security of instruments and access to the electrical grid. Approximately one third of the stations were installed in castle or chateau vaults; others were placed in churches or abandoned buildings. Sensors were placed on solid foundations such as concrete slabs or floors. The majority of the sites represent urban free-field conditions. Figure 5 shows examples of typical station installations.

Each station is equipped with thermally insulated broadband sensors (Streckeisen STS-2, Guralp CMG-40T, 3ESP(C), 3T, 6T; see Table S1 in the Supplement), offering corner periods between 30 s and 120 s (Fig. 4), and data acquisition system (DAS) GAIA developed by the Czech company VISTEC (24-bit, 130 dB dynamic range at a 100 Hz sampling rate). The stations are powered from the electrical grid and equipped with backup batteries. Communication and remote control are enabled by modems transmitting state-of-health (SOH) reports and supporting remote rebooting and mass centering (Vecsey et al., 2017). Data are sampled at 100 Hz, with precise timing guaranteed by the GPS receivers. Although the stations initially operated offline, they have been gradually upgraded to online transmission, with 26 of the 34 stations now operating in real time.

Figure 5. Examples of a castle site and installations of seismic stations from the MOBNET pool: (a) Castle Bítov hosting station A084A; (b) Exterior of castle Bítov, where the red arrow indicates the vault with the station; (c) Instrument setup at station SK14A in the cellar in Spišská Kapitula; (d, e) Double insulation of the sensor at station SK20A Baňa.

The seismic data are stored locally in the GAIA units and transmitted in real-time to IG CAS servers via the SeedLink protocol, which includes buffering to handle temporary outages. After automatic adjustment of network and location codes at IG CAS, the data are forwarded to the LMU node of the European Integrated Data Archive (EIDA; Strollo et al., 2021), ensuring rapid integration into the broad data-sharing infrastructure.

The State-of-Health (SOH) of each station (e.g., flash memory usage, GPS synchronization, battery voltage, temperature, and basic signal quality, e.g., offset or clipping) is monitored through daily SOH reports and online streams. Remote control capabilities allow operators to reboot communication devices and DAS units and to perform mass centering where supported. Routine maintenance visits include inspection of instrument condition, sensor centering, verification of spirit levels, basic calibration checks, and replacement of flash cards. Sensor orientations are measured with an accuracy better than $\pm 0.1°$ using a fiber-optic gyrocompass and are rechecked once a year. Data retrieved during maintenance are subject to quality control at IG CAS to correct potential issues (e.g., timing errors, polarity reversals, or gain inconsistencies; Vecsey et al., 2017) before the validated data replace online streams in the EIDA node.

2.2 Temporary stations of the University of Vienna (IMGW) deployed in Austria and Slovakia

The Department of Meteorology and Geophysics, University of Vienna (IMGW), contributes to the AdriaArray Seismic Network with 25 broadband stations. Except for station A004A, which was deployed in the Vienna Basin already in 2014, all other stations were initially installed for the AlpArray project (Hetényi et al., 2018a) between February and November 2015. Subsequently, the stations were transferred to the PACASE project in 2019 (Schlömer et al., 2024), and in 2022, they were integrated into the running AdriaArray Seismic Network.

Although the sites were originally designed for temporary deployment for three years only, regular maintenance has ensured that most stations remain operational to date. Their deployment is expected to continue until the summer of 2026, marking a decade of operation for the IMGW installations. Over the years, five stations had to be replaced due to high noise levels or security concerns. In such cases, the original "A" at the end of the station names was changed to "B". Moreover, at one original site (A006A), the wine cellar collapsed in 2021, and the station could not be rebuilt. At the other three sites, property owners did not extend the agreements for keeping the station for a longer time. Some temporary sites were later replaced by permanent stations of the Austrian OE network. All these adjustments occurred during the AlpArray project, and no additional relocations were needed during the PACASE (2019-2022) or AdriaArray (2022-2025). As a result, the network configuration has remained stable, with all 25 stations retaining their original AlpArray identifiers, comprising an "A," three digits, and either an "A" or "B" suffix – see magenta triangles in Fig. 3 and Table S1 in the Supplement. The IMGW stations previously included in the AlpArray and PACASE with network code Z3, currently incorporated in the AdriaArray, changed their network codes to 7B (AdriaArray Temporary Network, Austria, Croatia, Slovakia, 2022) on 1 January 2023.

Detailed descriptions of the network design, deployment, and site performance are given in Fuchs et al. (2015, 2016). Here, we provide a concise overview of the stations that continue to operate within the AdriaArray. The IMGW stations as a part of the AdA network span a diverse range of landscapes, including the Eastern Alps, the southernmost part of the Bohemian Massif, the Vienna Basin, the westernmost Carpathians, and the northern parts of the Pannonian Basin in Austria and Slovakia. Data quality varies across sites, with very quiet locations in the mountain regions and noisy ones in the basin areas. Most stations are installed in the basements of abandoned or rarely used buildings, forest huts and wine cellars. Some of the stations are located in castles, cemeteries, and military bunkers. Sensors are placed on solid concrete floors or on small concrete pillars constructed where necessary. Figure 6 shows the installation of station A011B as an example.

The network equipment is largely uniform, with both sensors and data acquisition systems provided by Reftek. Each seismic station includes the Reftek 151 "Observer" broadband sensor with a 60-second corner period (generations A and B with two variants, represented in the metadata by their respective poles and zeros) and a Reftek 130 or 130S acquisition unit. The digitizers provide a 24-bit dynamic range of >136 dB at 100 Hz sampling. Other components include continuous-mode Garmin/Reftek 130 GPS units, AVM FritzBox 6850 LTE modems for telemetry, charging switches, and up to two 100 Ah batteries, all housed in custom-designed waterproof boxes. Data are stored locally on two compact flash cards (8-32 GB).

Between 2021 and 2022, older industrial modems were progressively replaced with AVM FritzBox 6850 LTE consumer modems, connected via VPN to a virtual server running Reftek software, hosted by the ZID (Zentraler

Figure 6. Example of the installation of temporary stations in Austria: outside and inside views of station A011B Reinberg.

Informatikdienst Universität Wien). This transition significantly reduced downtimes due to modem failures, and connection interruptions are now rare. Since 2015, all stations have operated in an online regime, transmitting data via the GSM network to IMGW servers in Vienna using Reftek's proprietary RTPD protocol. GeoSphere Austria (formerly ZAMG) collects these data and forwards them to the EIDA node at the Orfeus Data Center (ODC, Netherlands). Occasional transmission gaps caused by weak GSM coverage are mitigated by manual data retrieval during maintenance visits and subsequent backfilling of the EIDA archive. Online connectivity also enables real-time monitoring of station SOH and remote adjustments of digitizer settings, as well as remote centering of sensors. Sensors are thermally insulated with microfleece-Primaloft textile covers enclosed in styrofoam boxes sealed to the floor or pillar to minimize air circulation. Most stations are powered from the electrical grid, only several stations rely on solar panels. A few stations were originally supported by fuel cells, one of which remains operational at A017A (Waidhofen a.d. Ybbs).

Re-measuring the sensor orientations by a fiber optic gyrocompass in 2016 revealed significant deviations from the geographical north. For cases where the misalignment exceeded 5°, the N and E channels were renamed as 2 and 3 to comply with the SEED standards. Precise orientations are documented in the station metadata.

2.3 Temporary stations deployed in the outer Carpathians (Poland)

The Polish segment of the AdriaArray seismic network began recording in August 2022 and was scheduled to operate for nearly three years. The temporary stations were initially deployed in 2019 for the PACASE experiment with network code ZJ (Hetényi et al., 2019; Schlömer et al., 2024), and most of them remained at their original sites for the AdriaArray project with network code changed to Y8 (Neagoe, 2022; see cyan triangles in Fig. 3). Three new stations (PL32A, PL33A, and PL34A) were installed particularly for the AdriaArray network. Additionally, data from three permanent seismic stations NIE, OJC, and KWP in the Outer Carpathians, belonging to the Polish Seismological Network, complement the dataset collected by the temporary AdriaArray stations.

Three institutions contributed to this network with instrumentation. The Institute of Geophysics, Polish Academy of Sciences (IG PAS), provided 10 Guralp CMG-6T seismometers (30-second corner period) paired with Guralp DM24S3EAM data acquisition systems. The Institute of Geophysics, University of Warsaw (IG UW), supplied 12 Reftek-130B data acquisition systems equipped with Reftek 151-120 "Observer" broadband sensors (120-second corner period). The University of Silesia in Katowice contributed with 7 Reftek systems of the same type, six with 120-second Reftek broadband sensors and one with a Reftek Colt 60-second sensor (Fig. 4). All stations record at 100 Hz with a dynamic range of 130 dB. The GPS receivers ensure precise timing for the recorded data.

Site selection aimed to balance requirements on a dense and homogeneous station distribution with low seismic noise, accessibility, security, reliable grid power, and strong mobile telecommunications. Stations have been installed in unused basements of buildings, outbuildings, or rarely used public utility structures, such as churches or foresters' lodges. Sensors were placed on solid surfaces like concrete or tiled flooring; in a few cases, a 5-cm-thick granite slab was built for additional stability.

The sensors are thermally insulated with styrofoam boxes at each site. Each station is powered by the electrical grid, supplemented by 12V backup batteries to ensure continuous operation during power outages. Near real-time data transfer is achieved through UMTS/LTE mobile network connections.

Precise sensor orientation with respect to geographical north is critical for three-component interpretation methods. Initial alignment involved GNSS-RTK measurements outside the building, transferred to the sensor using a MEMS accelerometer and gyroscope device. Orientation was subsequently refined using a fiber-optic gyrocompass with an accuracy of 0.1°. Accurate orientation values are included in the station metadata.

The recorded seismic data are stored in the internal memory of the data acquisition units (Guralp systems with 16 GB inbuilt flash memory and Reftek units with 2×16 GB CF cards) and simultaneously transmitted in near real-time to IG PAS servers via secure UMTS/LTE connections. SOH parameters, such as temperature, voltage, and mass positions, are also transmitted. The SeedLink transmission system employs buffering and automatic reconnection mechanisms to ensure data continuity during short-term communication outages. Data from Reftek units are transferred through a custom Raspberry Pi-based setup (Polkowski et al., 2016), sent in short blocks, and automatically converted to miniSEED format before being forwarded via SeedLink to the NIEP EIDA node, ensuring their rapid integration into the European data infrastructure. Occasional transmission gaps caused by longer connection losses are mitigated through manual data retrieval during maintenance visits and subsequent backfilling of the archive.

Remote control and monitoring of both the Guralp and Reftek units are managed with the use of their proprietary software interfaces, accessible via a web browser or SSH. These tools allow for real-time parameter checks, such as free storage space, mass positions, timing, voltages, and temperature, as well as the adjustment of recording settings. For Reftek systems, the control interface additionally enables mass centering, which can also be automatically triggered if mass voltage thresholds exceed a user-defined duration.

3. Network performance and data completeness

Figure 7 shows examples of the network's capability to record both a teleseismic event with magnitude Mw 7.4 and a local event with magnitude Mw 5.0. The clear phase arrivals are visible in the waveforms, which demonstrate the high performance of the network and data plausibility for the earthquake location and structural studies by different methods, e.g., by tomography, receiver functions, or shear-wave splitting. In Fig. 7, signals from permanent stations (in blue) and temporary stations (in yellow) are shown separately, highlighting the considerable improvement in detection capability achieved by the inclusion of the temporary AdriaArray stations. Notably, the densely spaced MOBNET stations in Slovakia significantly improved the event localization and particularly the depth estimation for the Humenné earthquake (Schlömer et al., 2024).

Approximately 2.8 TB of broadband seismic data, sampled at 100 Hz, were collected over a 30-month period between 20 May 2022 and 15 January 2025. However, the data completeness, as stored in EIDA (Fig. 8), is not consistent for all the stations. Some of the stations exhibit significant gaps. MOBNET stations achieve an average data completeness of 96%, despite some stations remaining offline and their data being delivered to EIDA with a delay. The data completeness of the Polish fully online temporary stations is high too, it attains 95%, on average. However, the data completeness in EIDA of the IMGW stations attains only 42%, on average, as of 15 January 2025.

Seismic data from the northern part of the AdriaArray network are accessible through the EIDA nodes. Since the beginning of the network installation in the AdriaArray in May 2022, the temporary stations have been operated under five different network codes (Fig. 8). Data from networks Z3 and 7B are hosted in the ODC EIDA node (https://www.orfeus-eu.org) and are openly accessible. The ZJ network, stored in the LMU EIDA node (https://erde.geophysik.uni-muenchen.de), follows the PACASE data policy and is available since July 2025. Networks with codes Y8 and Z6 contribute their data to the NIEP EIDA node (https://eida-sc3.infp.ro) and LMU EIDA node, respectively. Data from the Y8 and Z6 networks are subject to a two-year rolling embargo and thus, during the embargo period, accessible only for members of the AdriaArray Seismology Group except for monitoring and alerting local seismicity in the AdriaArray region.

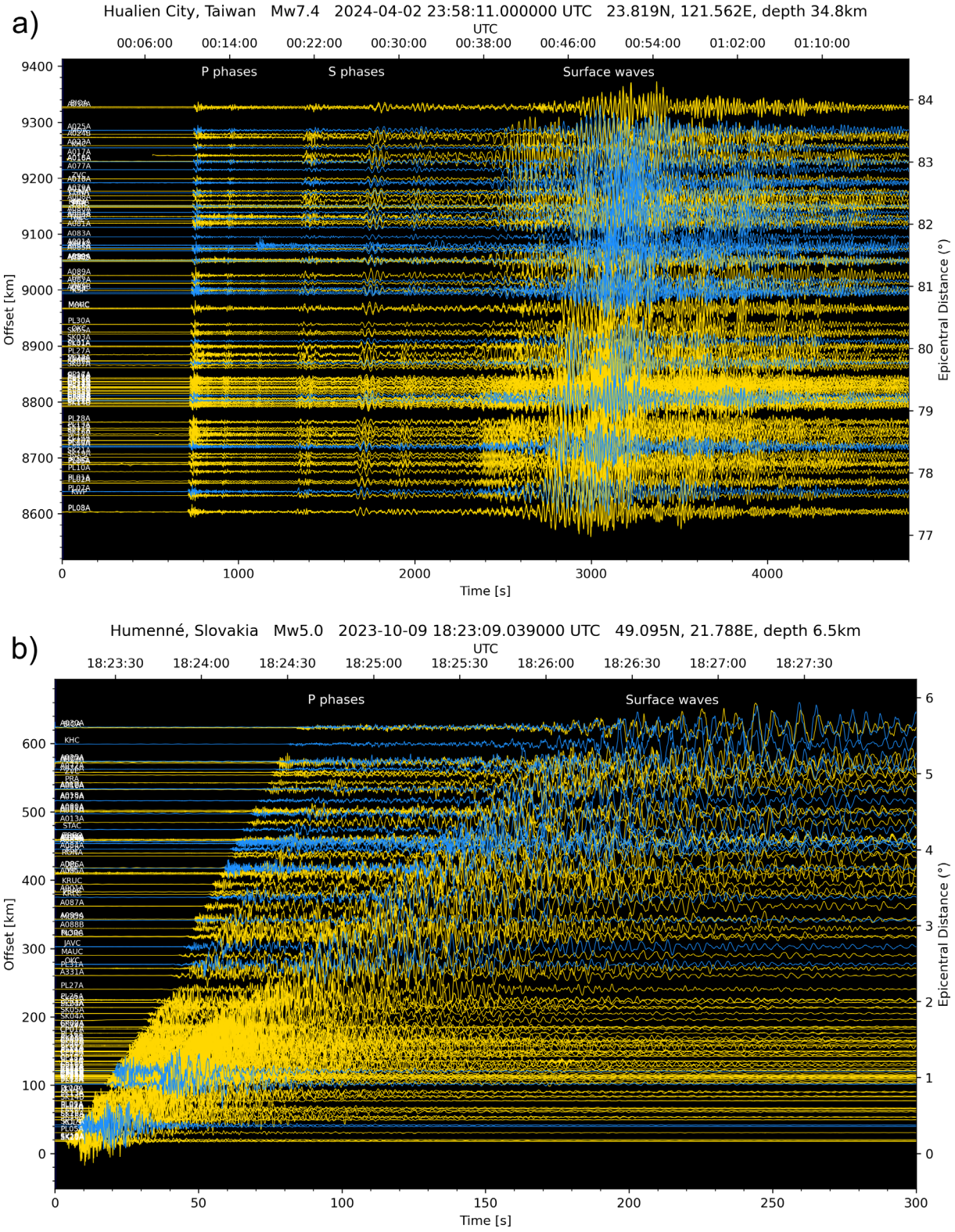

Figure 7. Examples of waveforms recorded in the northern part of the AdriaArray network: (a) teleseismic event located in Hualien City, Taiwan, originated on 2 April 2024, at 23:58:11 UTC with magnitude Mw = 7.4; (b) local event near Humenné, Slovakia, occurred on 9 October 2023, at 18:23:09 UTC with magnitude Mw = 5.0. Traces of temporary (yellow) and permanent (blue) stations are normalized to their maximum amplitudes; time on the lower axis refers to the earthquake origin time.

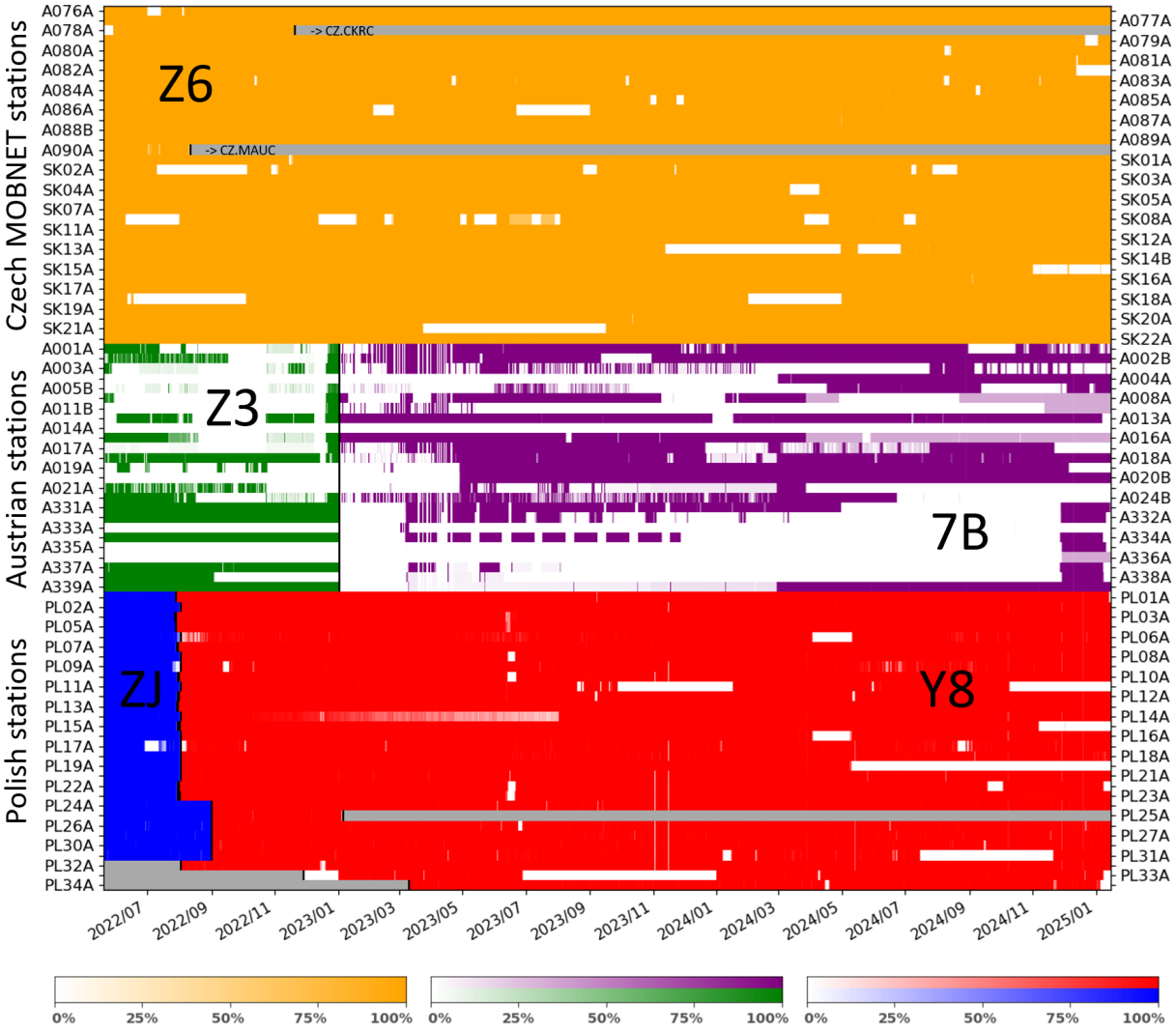

Figure 8. Data completeness at the EIDA nodes for the temporary stations of the northern part of the AdriaArray network from 20 May 2022 to 15 January 2025. The colors differentiate the stations from the MOBNET (orange), IMGW (green/purple), and Polish (blue/red) pools; 100% intensity of the colors stands for complete daily volumes of all three components; white color marks no data. Grey boxes – periods when stations have not been deployed.

4. Data quality and noise characteristics

To preserve the high accuracy and consistency of data recorded by the AdriaArray network, rigorous quality control procedures are of great importance. Each network operator contributing to AdA is responsible for data availability and quality, including regular maintenance, metadata correctness and completeness, and the use of data quality assurance tools. The same data-quality evaluation applied to the MOBNET pool (Vecsey et al., 2017) and the eastern Austrian and western Slovakian segments (Fuchs et al., 2016) during the AlpArray experiments is now also used for the AdA stations. A comprehensive description of data quality assessment across the AdA network is provided by Kolínský et al. (2025b).

Probabilistic power spectral densities (PPSD) represent an essential part of the data quality control workflow, as they provide a statistical representation of power spectral density variations over time (McNamara and Buland, 2004). The spectral densities offer valuable insights into typical noise levels and transient noise sources at each station. The PPSDs in different frequency bands reflect different noise sources: short-period noise (<1 s) is primarily influenced by local anthropogenic activity such as traffic and industrial operations, intermediate-period noise (1-20 s) is largely controlled by oceanic microseisms, and long-period noise (>20 s) is often driven by environmental factors such as wind or atmospheric pressure fluctuations (McNamara and Buland, 2004).

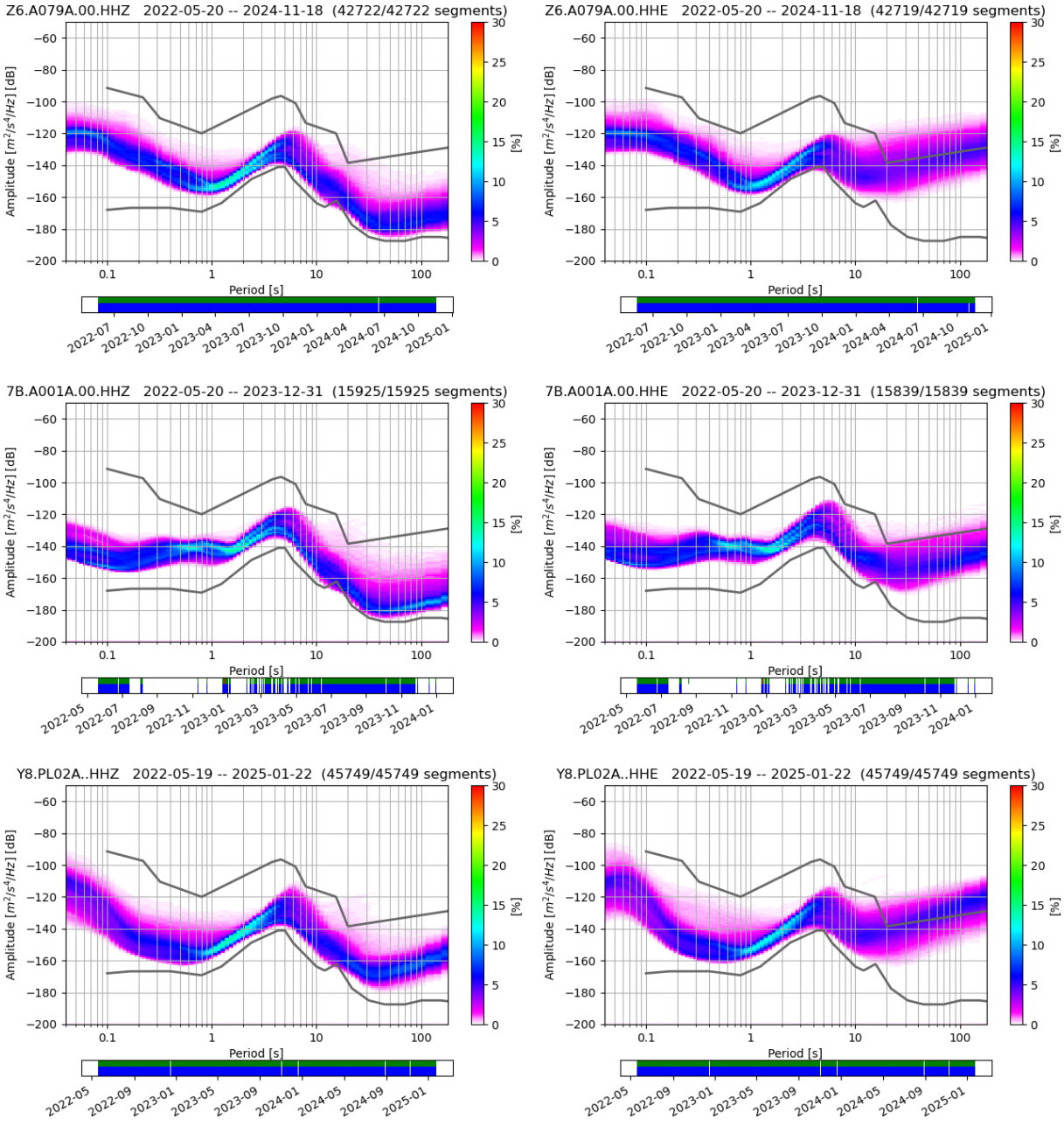

Figure 9. Examples of probabilistic power spectral densities (PPSD) for vertical and horizontal E-W components at stations A079A, A001A, and PL02A. The solid lines represent the NHNM and NLNM noise models (Peterson, 1993). All graphs were calculated for the period from 20 May 2022 to 15 January 2025, if available (data and PPSD availability below each graph in blue and green, respectively). PPSDs for all stations are presented in the Supplement material (Fig. S1).

We calculate and visualize all PPSDs using the ObsPy library (Krischer et al., 2015). The results are compared with the New High Noise Model (NHNM) and New Low Noise Model (NLNM) established by Peterson (1993). Vertical components of PPSDs for three stations shown in Fig. 9 are within the lower half of the NHNM-NLNM range, while long-period noise on the horizontal components is higher and sometimes exceeds the NHNM limit. The increase is attributed to the less convenient conditions of temporary deployments compared to the conditions of installation of permanent stations. PPSD plots for all temporary stations in the northern part of the AdriaArray network are available in the Supplementary materials (Fig. S1).

The medians of the PPSDs for the vertical and horizontal E-W components (Fig. 10), calculated from 20 May 2022 to 15 January 2025, show that the noise levels on both vertical and horizontal components remain below

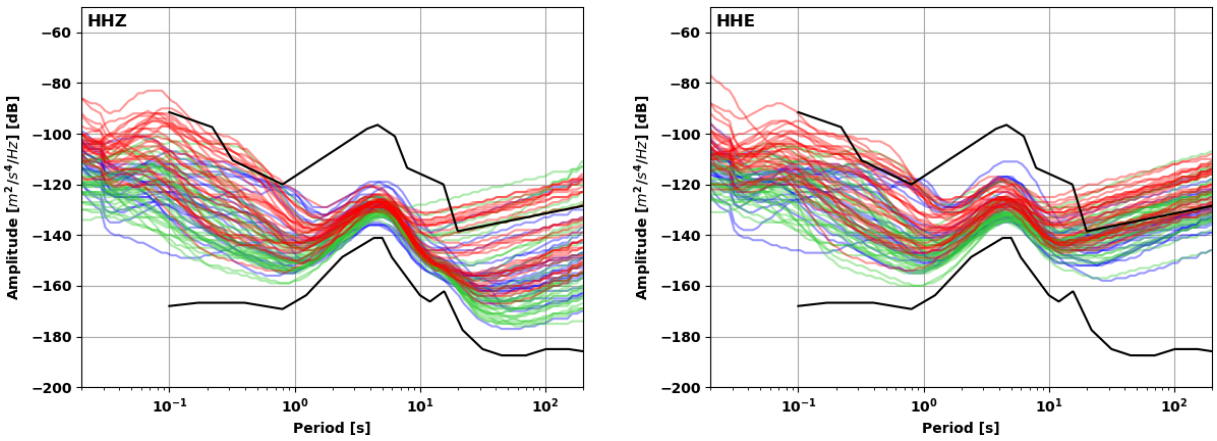

Figure 10. Median curves of probabilistic power spectral densities (PPSD) for vertical and horizontal E-W components, calculated for all temporary stations in the period from 20 May 2022 to 15 January 2025. The curves are color-coded by the institutions: IMGW station in the Vienna Basin and western Slovakia (blue), stations of the MOBNET pool in the Bohemian Massif and central and eastern Slovakia (green), and stations of the Polish group in the Outer Carpathians (red). The black lines correspond to the NHNM and NLNM models (Peterson, 1993).

the NHNM threshold for most of the stations at short periods (<1 s). However, some stations in Poland, located in the lowland highly-populated areas with industrial activity, exhibit elevated anthropogenic noise, occasionally exceeding the NHNM. Nevertheless, the requirement of homogeneous coverage of the region also forced us to select sites with higher noise. In the intermediate period range (1-10 s), noise levels across the network remain at the lower half of the model band. At long periods (>10 s), instrumental noise and effects of sensor tilts, caused by temperature and pressure fluctuations, become more pronounced. Unlike permanent seismic stations, which are typically housed in purposely built vaults with optimized environmental shielding, temporary stations deployed in field conditions suffer from worse environmental conditions. Therefore, long-period noise levels at some temporary sites exceed the NHNM, particularly on horizontal components.

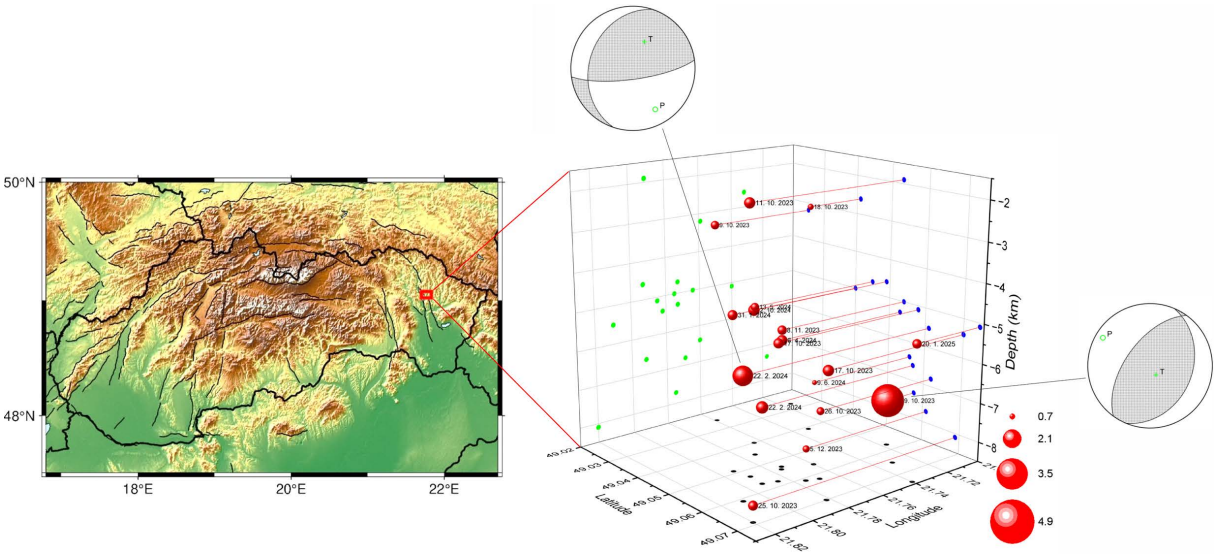

Figure 11. Seismic activity in eastern Slovakia between 9 October 2023 and 30 January 2025, monitored by AdA stations, along with focal mechanisms of the two strongest events. The first event (right) occurred on 9 October 2023 (see AdA waveforms in Fig. 7b) with a magnitude of M 5.0, a strike of 18.7°, a dip of 32.9°, and a rake of 75.2°. The second, weaker event (top) had a magnitude of M 2.7 and occurred on 22 February 2024 at 12:54:15 UTC, with a strike of 199°, a dip of 36°, and a rake of 8°.

5. Examples of data usage (preliminary results)

To illustrate the efficiency of the AdA network, we present examples of advanced seismic data processing. As the first example, we show the power of the AdA data for monitoring seismic activity in eastern Slovakia. Including the AdA data in the routine service of ESI SAS (Earth Science Institute of the Slovak Academy of Sciences, Department of Seismology) allowed us to locate the mainshock (Mw 5.0, NEIC) – the strongest event known in this region – together with 19 aftershocks down to a magnitude of 0.7 over the following ~15 months. We were also able to estimate focal mechanisms from first-motion polarities for some of these events (Fig. 11). We determined the mechanism of the strongest event occurred on 9 October 2023 (see the AdA waveforms in Fig. 7b) to have strike 18.7°, dip 32.9°, and rake 75.2° (see also Schlömer et al., 2024). The focal mechanism of the weaker event on 22 February 2024 exhibits strike 199°, dip 36°, and rake 8°. For this aftershock, polarities at seven temporary stations (SK15-17 and SK19-22) around the epicenter have been used. Five of them are within a radius of ~50 km, two of them up to 100 km to the SW. Unfortunately, more distant stations toward the east are missing. This situation accelerated discussions on closer cooperation between ESI SAS and the Institute of Geophysics in Kyiv (Ukraine) focused on the exchange of seismic data.

We also present here preliminary results of Moho depth estimates from the P receiver functions (PRF) in the Western Carpathians and the Bohemian Massif (Fig. 12) with the use of data from several passive seismic experiments running in the region since 1995 (Plomerová, 2025) – including AdriaArray, PACASE, and AlpArray from the more recent. We selected events with magnitude at least as the cut-off magnitude Mc by Liu and Gao (2010) and the signal-noise ratio (SNR) ≥2.5. The records were rotated into the LQT coordinate system and filtered with the band-pass filter 1-8 s. To remove source side effects, we followed the procedure of Kind et al. (1995) and Kind and Juan (2011), in which the horizontal components are deconvolved with the vertical ones (Berkhout, 1977) and stacked. We calculated the Moho depths by migrating the Ps delay times on the stacked PRF traces according to the IASP91 velocity model. The map in Fig. 12 is constructed from the high-quality PRF at 171 stations, the vast majority of which (72%) have more than 100 traces in the case of temporary stations and up to 1990 traces at permanent

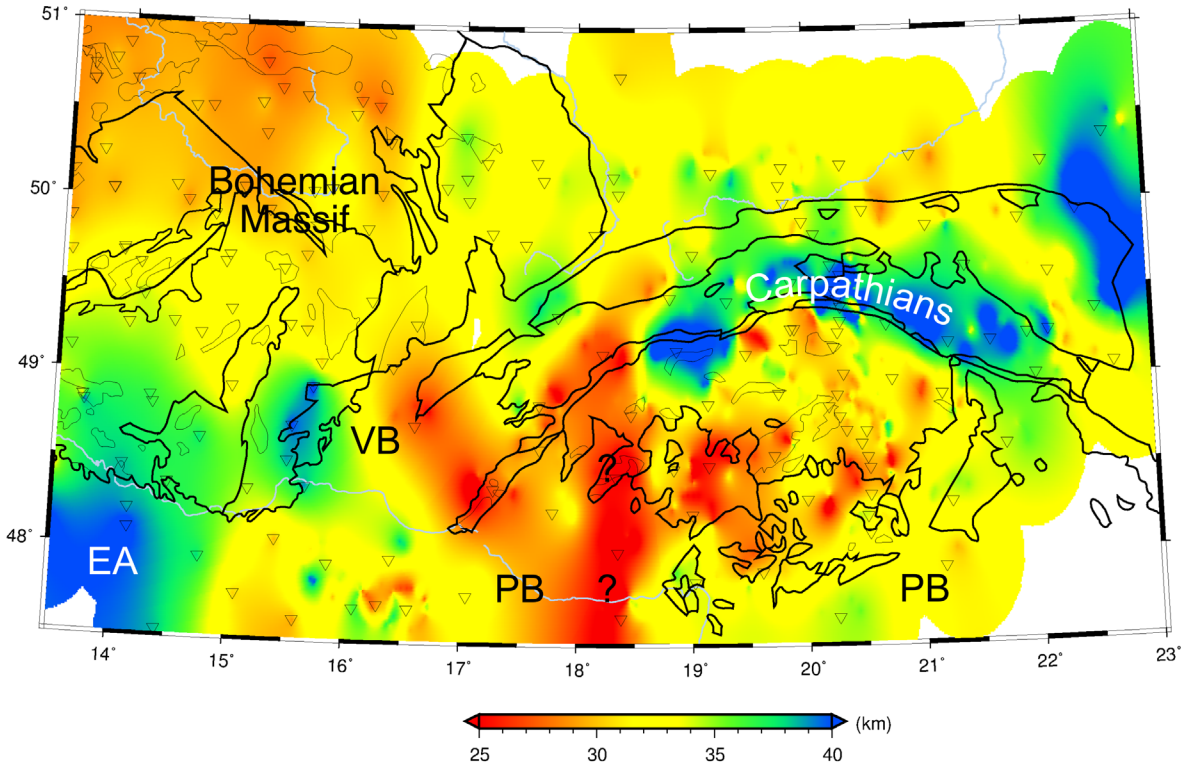

Figure 12. The Moho depth in the Western Carpathians and the eastern part of the Bohemian Massif estimated from P receiver functions from data of the AdriaArray, PACASE, AlpArray data, and several earlier experiments in the case of the Bohemian Massif (for more details see Kvapil et al., 2021). Abbreviations: EA – Eastern Alps, VB – Vienna Basin, PB – Pannonian Basin.

stations. On average, 287 traces per station have been used for the first Moho depth estimate. The distinct band of the deep Moho, east of the 19°E, follows the arcuate shape of the Western Carpathians. Similarly, a thick crust but with clearly southward dipping Moho characterizes the southern BM (Hetényi et al., 2018b). A standard depth of ~32-33 km is characteristic of the outer Carpathians in Poland, in the inner Carpathians, and in the eastern part of the BM. The crust thins significantly in the basins, though in some parts, e.g., in the Little Carpathians (~16°E), the extremely shallow values need to be verified with more data.

Shear-wave splitting analysis in the broader Western Carpathians region provides an example of the use of AdA data to constrain the upper-mantle structure. We applied the MFAST code (Savage et al., 2010; Teanby et al., 2004) to examine seismic anisotropy in the mantle beneath the region. The code implements the eigenvalue method for calculation of shear-wave splitting parameters (the delay time and fast polarization azimuth) with the assumption of a single-layer anisotropy (Silver and Chan, 1991). In this study, we use the recorded waveforms of the core-mantle-refracted shear SKS phases with the SNR ≥3 from earthquakes with magnitudes M > 5.5 and epicentral distances between 85° and 130° that occurred between 1 June 2022 and 31 January 2025. Several stages of data selection and quality control (Vecsey et al., 2017) were applied, both to the waveforms before the proper calculation of splitting parameters and to the results. First, the data were filtered using 16 different band-pass

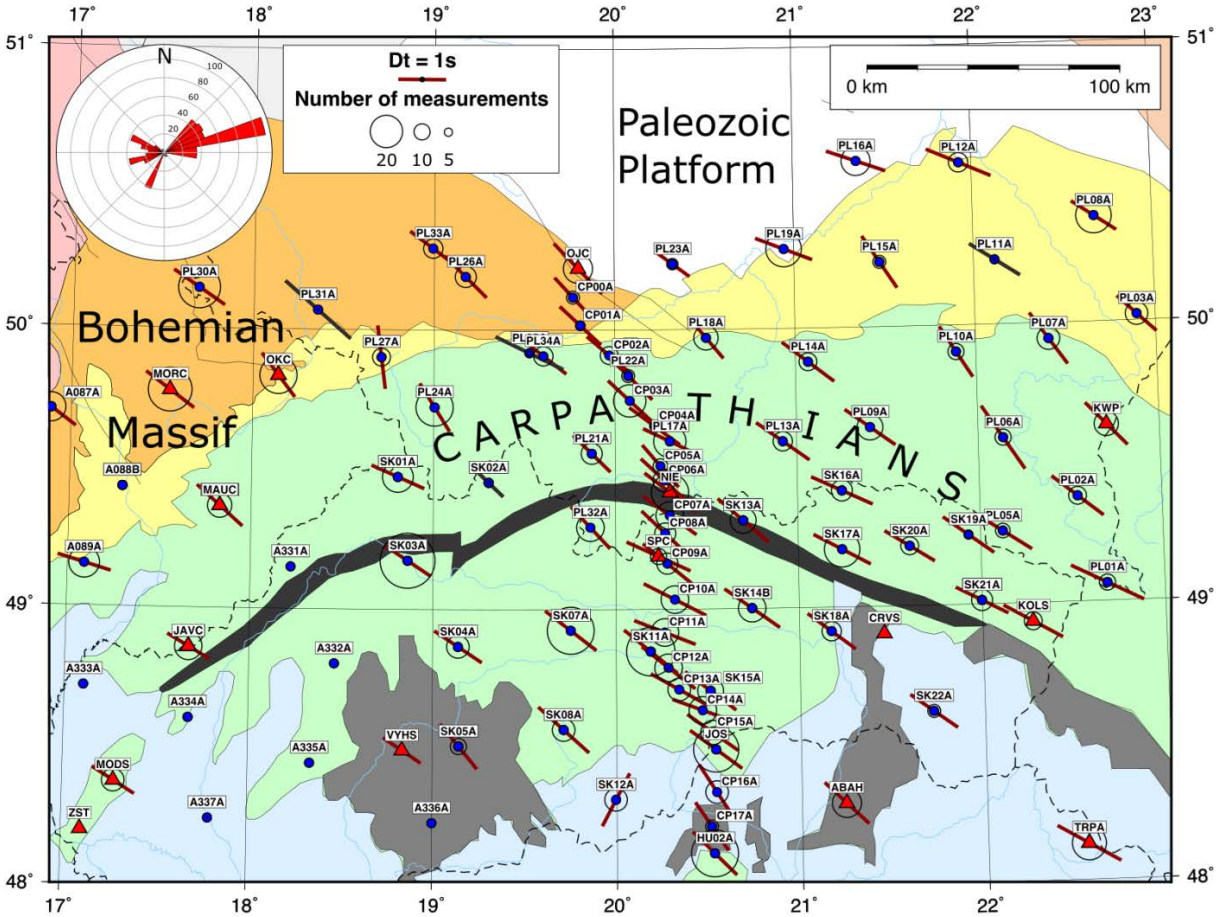

Figure 13. The average time delays and fast polarization azimuths (dark red bars oriented mostly NW-SE) at stations of the AdriaArray in the Western Carpathians, derived from SKS splitting analysis using the MFAST code (Savage et al., 2010; Teanby et al., 2004). Only measurements rated as "good", with the back-azimuth distribution showed in the histogram (inset in the upper left), are considered in the averages. The size of the black circles is proportional to the number of individual measurements used for averaging. The length of the bars is proportional to the average time delays of the slow split shear waves. The bars in dark grey indicate averages based on only three or fewer measurements. The thick black curve – Pieniny Klippen Belt (PKB); the light green areas north and south of the PKB – the Outer Carpathians and Inner Carpathians, respectively; the yellow – the Carpathian foredeep; the dark grey areas – Neogene volcanics; light blue – sediments of the Pannonian Basin; orange – Upper Silesia unit of the BM. Red triangles stand for permanent stations and blue circles for temporary stations of the AdriaArray.

filters with lower corner frequencies of 0.033, 0.05, 0.067, 0.1 Hz and higher corner frequencies of 0.2, 0.33, 0.5, and 1.0 Hz. For each filter, the SNR was calculated in a −20 s to 20 s time windows around the SKS arrival. The filter maximizing the product of the SNR and the filter bandwidth was then used for further analysis. The dominant period of the SKS phase was used as the base length of the time window for the splitting analysis. This window was then systematically adjusted by shifting its start time in 5 increments and its end time in 25 increments. In this way, splitting parameters were calculated for 125 different test windows, whose lengths varied from one dominant period to twice that value. The computation was performed using a grid-search algorithm that minimizes the smallest eigenvalue of the particle-motion covariance matrix. To estimate the solution uncertainty, we determine the 95% confidence interval with the use of an F-test. In order to determine the most stable solution, all results were clustered (Teanby et al., 2004). The cluster with the minimum total variance of results was considered optimal. In this cluster, the measurement with the minimum variance of the splitting parameters was selected as the best solution. Figure 13 reveals the largely consistent NW-SE pattern of the station-averaged fast polarization azimuths, with only minor variations in the delay times. The general uniformity in the fast polarization azimuths implies a stable anisotropic fabric in the upper mantle beneath the region, at first glance. However, more detailed three-dimensional splitting analysis (Šílený and Plomerová, 1996; Vecsey et al., 2008) and integrated body-wave analysis (Plomerová et al., 2012) need to be applied to larger data sets. Complete results of the shear-wave splitting, receiver functions, etc., will be presented in separate papers.

6. Concluding remarks

Scientists from institutions in four countries (the Czech Republic, Poland, Austria, and Slovakia) collaborated on station installation and maintenance, data collection and quality control, and the provision of the recorded data from the northern promontory of the AdriaArray to the EIDA nodes. Altogether, 89 temporary broadband stations covered the southeastern part of the Bohemian Massif, the Eastern Alps, the Western Carpathians, and the northernmost part of the Pannonian Basin, complementing thus 31 broadband permanent stations operated in the region by then. Since the start of the AdriaArray in spring 2022, 2.8 TB of, in general, high-quality data has been archived in the EIDA nodes by 15 January 2025, with an average completeness of ~96% for the temporary stations from the MOBNET and the Polish pools. Moreover, 91% of stations operate in real-time mode at the moment. The high-quality data recorded in the northern promontory of the AdA network will contribute to a wide range of research tasks, including the structural imaging of the crust and the upper mantle or plate deformation and its relation to seismic hazard among others.

Data availability statement. Waveform data from all AdriaArray stations are available through ORFEUS EIDA. Data from the permanent stations and from temporary stations with network codes 7B, Z3, and ZJ are publicly accessible immediately. Data from temporary stations with network codes Y8 and Z6 are freely available to the AdriaArray Seismology Group participants. According to the data embargo policy applied to these two temporary networks, the data will be made publicly accessible after a two-year delay. However, all data are immediately available for monitoring and alerting of local seismicity in the AdriaArray region.

Acknowledgements. The deployment of stations of the MOBNET pool of the Institute of Geophysics of the Czech Academy of Sciences (IG CAS), the fieldwork of IG CAS members, and research were supported by grants No. 21-25710S and No. 23-06370S of the Grant Agency of the Czech Republic, and by the programme Strategy AV21 'Dynamic Planet Earth' funded by the Czech Academy of Sciences. The performance of the MOBNET pool was partly supported by the Operational Programme Research, Development and Education of the Ministry of Education, Youth and Sports of the Czech Republic, CzechGeo/EPOS-Sci CZ.02.1.01/0.0/0.0/16_013/0001800. We appreciate access to CESNET storage facilities provided by the project 'e-Infrastructure CZ' under the programme 'Projects of Large Research, Development, and Innovations Infrastructures' LM2018140. The Polish research group has been supported by the National Science Centre, Poland (agreement no. UMO-2019/35/B/ST10/01628). The Slovak research group has been supported by the Slovak Foundation Grant VEGA 2/0163/25 and by the Slovak Research and Development Agency Grant APVV-21-0159; LF has been partly funded by the Institutional Research Plan RVO67985891 of the Institute of Rock Structure and Mechanics of the Czech Academy of Sciences.

Maps were plotted using the Generic Mapping Tools (GMT; Wessel et al., 2013). The Python toolbox ObsPy (Krischer et al., 2015) was used for data download, processing, and visualization.

References

AdriaArray Temporary Network, Austria, Croatia, Slovakia (2022). Data set, network code 7B.

AlpArray Seismic Network (2015). AlpArray Seismic Network (AASN) temporary component, AlpArray Working Group, doi:10.12686/alparray/z3_2015.

Amante, C. and B. W. Eakins (2009). ETOPO1 1 Arc-Minute Global Relief Model: Procedures, Data Sources and Analysis, NOAA Technical Memorandum NESDIS NGDC-24, National Geophysical Data Center, NOAA, doi:10.7289/V5C8276M.

Berkhout, A. J. (1977). Least-squares inverse filtering and wavelet deconvolution, Geophysics, 42, 7, 1369-1383, doi:10.1190/1.1440798.

Borleanu, F., L. Petrescu, C. Neagoe, H. Kampfová Exnerová et al. (2025). The AdriaArray Temporary Broadband Network in Romania: Enhancing Seismic Monitoring and Data Quality, Ann. Geophys., 68, this issue, doi:10.4401/ag-9318.

Cipciar, A., K. Csicsay, M. Kristeková, L. Fojtíková et al. (2025). Slovak Earthquakes Catalogue, Version 2025, Earth Science Institute of the Slovak Academy of Sciences.

Danciu, L., S. Nandan, C. Reyes, R. Basili et al. (2021). The 2020 update of the European Seismic Hazard Model: Model Overview, EFEHR Technical Report 001, v1.0.0, doi:10.12686/a15.

ESI SAS, former GPI SAS – Geophysical Institute of the Slovak Academy of Sciences (2004). National Network of Seismic Stations of Slovakia, Data set, GFZ Data Services, doi:10.14470/FX099882.

Faccenna, C., T. W. Becker, L. Auer, A. Billi et al. (2014). Mantle dynamics in the Mediterranean, Rev. Geophys., 52, 283-332, doi:10.1002/2013RG000444.

Fuchs, F., P. Kolínský, G. Gröschl, M. T. Apoloner et al. (2015). Site selection for a countrywide temporary network in Austria: noise analysis and preliminary performance, Adv. Geosci., 41, 25-33, doi:10.5194/adgeo-41-25-2015.

Fuchs, F., P. Kolínský, G. Gröschl, G. Bokelmann et al. (2016). AlpArray in Austria and Slovakia: technical realization, site description and noise characterization, Adv. Geosci., 43, 1-13, doi:10.5194/adgeo-43-1-2016.

Golonka, J., A. Waskowska and A. Slaczka (2019). The Western Outer Carpathians: Origin and evolution, Z. Dtsch. Ges. Geowiss., 170, 3-4, 229-254, doi:10.1127/zdgg/2019/0193.

Handy, M. R., K. Ustaszewski and E. Kissling (2015). Reconstructing the Alps-Carpathians-Dinarides as a key to understanding switches in subduction polarity, slab gaps and surface motion, Int. J. Earth Sci., 104, 1-26, doi:10.1007/s00531-014-1060-3.

Handy, M. R., J. Giese, S. M. Schmid, J. Pleuger et al. (2019). Coupled Crust-Mantle Response to Slab Tearing, Bending, and Rollback Along the Dinaride-Hellenide Orogen, Tectonics, 38, 8, 2803-2828, doi:10.1029/2019TC005524.

Hetényi, G., I. Molinari, J. Clinton, G. Bokelmann et al. (2018a). The AlpArray seismic network: a large-scale European experiment to image the Alpine Orogen, Surv. Geophys., 39, 1009-1033, doi:10.1007/s10712-018-9472-4.

Hetényi, G., J. Plomerová, I. Bianchi, H. Kampfová Exnerová et al. (2018b). From mountain summits to roots: Crustal structure of the Eastern Alps and Bohemian Massif along longitude 13.3°E, Tectonophysics, 744, 239-255, doi:10.1016/j.tecto.2018.07.001.

Hetényi, G., J. Plomerová, M. Bielik, G. Bokelmann et al. (2019). Pannonian-Carpathian-Alpine Seismic Experiment, Data set, International Federation of Digital Seismograph Networks, doi:10.7914/SN/ZJ_2019.

van Hinsbergen, D. J. J., T. H. Torsvik, S. M. Schmid, L. C. Maţenco et al. (2020). Orogenic architecture of the Mediterranean region and kinematic reconstruction of its tectonic evolution since the Triassic, Gondwana Res., 81, 79-229, doi:10.1016/j.gr.2019.07.009.

Hók, J., O. Pelech, F. Teťák, Z. Nemeth et al. (2019). Outline of the geology of Slovakia (W. Carpathians), Min. Slov., 51, 1, 31-60.

Institute of Geophysics of the Czech Academy of Sciences-CAS, Charles University, Prague, Institute of Geonics, CAS, Institute of Physics of the Earth, Masaryk University and Institute of Rock Structure and Mechanics, CAS (1973). Czech Regional Seismic Network, Data set, International Federation of Digital Seismograph Networks, doi:10.7914/SN/CZ.

Institute of Geophysics, Polish Academy of Sciences (1990). Polish Seismological Network, Data set, International Federation of Digital Seismograph Networks, doi:10.7914/90rh-0q80.

Kampfová Exnerová, H., L. Dimitrova, T. Nagel, L. Dimova et al. (2025). AdriaArray experiment on the territory of Bulgaria, Ann. Geophys., 68, this issue, doi:10.4401/ag-9295.

Kästle, E. D., C. Rosenberg, L. Boschi, N. Bellahsen et al. (2020). Slab break-offs in the Alpine subduction zone, Int. J. Earth Sci., 109, 587-603, doi:10.1007/s00531-020-01821-z.

Kind, R., G. L. Kosarev and N. V. Petersen (1995). Receiver functions at the stations of the German Regional Seismic Network (GRSN), Geophys. J. Int., 121, 1, 191-202, doi:10.1111/j.1365-246X.1995.tb03520.x.

Kind, R. and X. Yuan (2011). Seismic receiver function technique, in Encyclopaedia of Solid Earth Geophysics H. K. Gupta (Ed.), Encyclopaedia of Earth Sciences Series, Springer, Dordrecht.

Kissling, E. (2024). Adria microplate: a puzzling key stone in west-central Mediterranean geodynamics, Ann. Geophys., 67, 4, doi:10.4401/ag-9160.

Kolínský, P., T. Meier, M. Agius, A. Bijedić et al. (2025a). AdriaArray – a Passive Seismic Experiment to Study Structure, Geodynamics and Geohazards of the Adriatic Plate, Ann. Geophys., 68, this issue, doi:10.4401/ag-9284.

Kolínský, P., J. Stampa, L. Vecsey, F. Eckel et al. (2025b). Methods for data and metadata quality tests of large dense seismic networks – focus on AdriaArray, Ann. Geophys., 68, this issue, doi:10.4401/ag-9328.

Krischer, L., T. Megies, R. Barsch, M. Beyreuther et al. (2015). ObsPy: a bridge for seismology into the scientific Python ecosystem, Comput. Sci. Discov., 8, 014003, doi:10.1088/1749-4699/8/1/014003.

Kvapil, J., J. Plomerová, H. Kampfová Exnerová, V. Babuška et al. (2021). Transversely Isotropic Lower Crust of Variscan Central Europe imaged by Ambient Noise Tomography of the Bohemian Massif, Solid Earth, 12, 5, 1051-1074, doi:10.5194/se-12-1051-2021.

Liu, K. H. and S. S. Gao (2010). Spatial variations of crustal characteristics beneath the Hoggar swell, Algeria, revealed by systematic analyses of receiver functions from a single seismic station, Geochem. Geophys. Geosyst., 11, Q08011, doi:10.1029/2010GC003091.

McNamara, D. E. and R. P. Buland (2004). Ambient Noise Levels in the Continental United States, Bull. Seism. Soc. Am., 94, 4, 1517-1527, doi:10.1785/012003001.

Neagoe, C. (2022). AdriaArray Temporary Network: Bulgaria, Moldova, Poland, Romania, Ukraine, Data set, International Federation of Digital Seismograph Networks, doi:10.7914/b1sc-0n71.

Peterson, J. (1993). Observations and modeling of seismic background noise, USGS Open-File report, 93-322.

Plomerová, J., L. Vecsey and V. Babuška (2012). Mapping seismic anisotropy of the lithospheric mantle beneath the northern and eastern Bohemian Massif (central Europe), Tectonophysics, 564, 38-53, doi:10.1016/j.tecto.2011.08.011.

Plomerová, J. (2025). MOBNET pool of transportable seismic stations in European passive experiments, Ann. Geophys., 68, this issue, doi:10.4401/ag-9266.

Polkowski, M., B. Plesiewicz, J. Wiszniowski, M. Wilde Piórko et al. (2016). Local Seismic Events in the Area of Poland Based on Data from the PASSEQ 2006-2008 Experiment, Acta Geophys., 64, 4, 2091-2112, doi:10.1515/acgeo-2016-0091.

Savage, M. K., A. Wessel, N. A. Teanby and A. W. Hurst (2010). Automatic measurement of shear wave splitting and applications to time varying anisotropy at Mount Ruapehu volcano, New Zealand, J. Geoph. Res. Sol. Ea., 115, 3430-3458, B12321, doi:10.1029/2010JB007722.

Schmid, S. M., B. Fügenschuh, A. Kounov, L. Maţenco et al. (2020). Tectonic units of the Alpine collision zone between Eastern Alps and western Turkey, Gondwana Res., 78, 308-374, doi:10.1016/j.gr.2019.07.005.

Schlömer, A., J. Wassermann, J. Plomerová, L. Vecsey et al. (2022). AdriaArray Temporary Network: Albania, Austria, Czech Rep., Germany, Hungary, Kosovo, Montenegro, Slovakia, Data set, International Federation of Digital Seismograph Networks, doi:10.7914/2cat-tq59.

Schlömer, A., G. Hetényi, J. Plomerová, L. Vecsey et al. (2024). The Pannonian-Carpathian-Alpine seismic experiment (PACASE): network description and implementation, Acta Geod. Geophys., 59, 249-270, doi:10.1007/s40328-024-00439-w.

Šílený, J. and J. Plomerová (1996). Inversion of shear-wave splitting parameters to retrieve three-dimensional orientation of anisotropy in continental lithosphere, Phys. Earth Planet. Inter. , 95, 3-4, 277-292, doi:10.1016/0031-9201(95)03121-9.

Silver, P. G. and W. W. Chan (1991). Shear wave splitting and subcontinental mantle deformation, J. Geophys. Res., 96, 16429-16454, doi:10.5194/se-5-779-2014.

Soni, T., C. Schiffer, S. Mazur, M. Mikołajczak et al. (2025). A dense seismological profile through the western Carpathians – new insights into Earth's structure, geodynamic evolution and seismicity, Ann. Geophys., 68, this issue, doi:10.4401/ag-9273.

Strollo, A., D. Cambaz, J. Clinton, P. Danecek et al. (2021). EIDA: The European Integrated Data Archive and Service Infrastructure within ORFEUS, Seismol. Res. Lett., 92, 3, 1788-1795, doi:10.1785/0220200413.

Teanby, N. A., J. M. Kendall and M. Van der Baan (2004). Automation of shear-wave splitting measurements using cluster analysis, B. Seismol. Soc. Am., 94, 2, 453-463, doi:10.1002/2014JB011665.

Tozer, B., D. T. Sandwell, W. H. F. Smith, S. C. Olsen et al. (2019). Global bathymetry and topography at 15 arc sec:SRTM15+, Earth Space Sci., 6, 10, 1847-1864, doi:10.1029/2019ea000658.

Vecsey, L., J. Plomerová and V. Babuška (2008). Shear-wave splitting measurements – Problems and solutions, Tectonophysics, 462, 178-196, doi:10.1016/j.tecto.2008.01.021.

Vecsey, L., J. Plomerová, P. Jedlička, H. Munzarová et al. (2017). Data quality control and tools in passive seismic experiments exemplified on the Czech broadband seismic pool MOBNET in the AlpArray collaborative project, Geosci. Instrum. Method. Data Syst., 6, 505-521, doi:10.5194/gi-6-505-2017.

Wessel, P., W. H. F. Smith, R. Scharroo, J. Luis et al. (2013). Generic Mapping Tools: improved version released, EOS Trans. AGU, 94, 45, 409-410, doi:10.1002/2013EO450001.

ZAMG – Zentralanstalt für Meteorologie und Geodynamik (1987). Austrian Seismic Network, Data set, FDSN, doi:10.7914/SN/OE.

***CORRESPONDING AUTHOR: Luděk VECSEY**,
Institute of Geophysics of the Czech Academy of Sciences, Prague, Czech Republic
e-mail: vecsey@ig.cas.cz